REGULAR ARTICLE

Enriched environment and physical activity reduce microglia and influence the fate of NG2 cells in the amygdala of adult mice

Dan Ehninger · Li-Ping Wang · Friederike Klempin · Benedikt Römer · Helmut Kettenmann · Gerd Kempermann

Abstract Proliferative cells expressing proteoglycan neuron-glia 2 (NG2) are considered to represent parenchymal precursor cells in the adult brain and are thought to differentiate primarily into oligodendrocytes. We have studied cell genesis in the adult amygdala and found that, up to 1 year after the labeling of proliferating cells with bromodeoxyuridine, most proliferating NG2 cells remain NG2 cells, and only a few slowly differentiate into mature oligodendrocytes, as assessed by the expression of 2',3'-cyclic nucleotide 3'-phosphodiesterase. We have detected no signs of neurogenesis but have confirmed the expression of "neuronal" markers such as Doublecortin in NG2 cells. Nestin-expressing NG2 cells in the amygdala show electrophysiological properties known for oligodendrocyte precursor cells in the corpus callosum. Application of the glutamate agonist kainate elicits a "complex" response consisting of a rapid and long-lasting blockade of the resting K^+ conductance, a transient cationic current, and a transient increase of an outwardly directed K^+ conductance, suggesting the responsiveness of NG2 cells to excitation. Proliferation of NG2 cells increases in response to behavioral stimuli of activity, voluntary wheel running, and environmental enrichment. In addition to reducing the number of newborn microglia, behavioral activity results in a decrease in S100β-expressing newborn NG2 cells in the amygdala. Because S100β expression in NG2 cells ceases with oligodendrocyte maturation, this finding suggests that NG2 cells in the amygdala undergo activity-dependent functional alterations, without resulting in a measurable increase in new mature oligodendrocytes over the time

Dan Ehninger and Li-Ping Wang contributed equally to this work.

D. Ehninger (✉)
DZNE, German Center for Neurodegenerative Diseases,
53175 Bonn, Germany
e-mail: dan.ehninger@dzne.de

L.-P. Wang
Shenzhen Key Lab of Neuropsychiatric Modulation,
Shenzhen Institutes of Advanced Technology,
Chinese Academy of Sciences,
Shenzhen 518055, China

F. Klempin
University of Washington,
Institute for Stem Cell
and Regenerative Medicine,
Seattle, WA 98109, USA

B. Römer
University Hospital Stavanger, Division of Psychiatry,
Stavanger, Norway

H. Kettenmann
Max Delbrück Center for Molecular Medicine
(MDC) Berlin-Buch,
Robert-Rössle-Strasse 10,
13125 Berlin, Germany

G. Kempermann
DZNE, German Center for Neurodegenerative Diseases,
01307 Dresden, Germany

G. Kempermann (✉)
CRTD – Center for Regenerative Therapies Dresden,
01307 Dresden, Germany
e-mail: gerd.kempermann@crt-dresden.de

period covered by the present study. The adult amygdala thus shows signs of mixed activity-dependent plasticity: reduced numbers of microglia and, presumably, an altered fate of NG2 cells.

Introduction

The addition of new neurons to the adult dentate gyrus is emerging as an important aspect of the structural plasticity that serves as a basis for hippocampus-dependent learning and memory processes (Deng et al. 2010). In the dentate gyrus, new neurons are generated from dividing precursor cells in the subgranular zone in a multi-step process that underlies complex regulation through behavioral and environmental factors. Outside the hippocampus (and the second neurogenic region in the subventricular zone and olfactory bulb), consistent evidence for constitutive adult neurogenesis is lacking. Nevertheless, throughout the brain, considerable *de novo* cell formation occurs in the gray and white matter. This cell genesis is generally thought to affect primarily oligodendrocytes (Levison et al. 1999). The physiological significance of this phenomenon is poorly understood. In the neocortex, physiological paradigms of behavioral activity, voluntary wheel running, and environmental enrichment, all of which robustly induce adult hippocampal neurogenesis, can additionally induce gliogenesis and the proliferation of resident microglia in the cortex (Ehninger and Kempermann 2003). The same stimuli also induce the proliferation of astrocytes in the non-neurogenic hippocampal area CA1 (Kronenberg et al. 2007). The possible involvement of these behavioral paradigms in the regulation of the *de novo* cell formation in other brain structures and the physiological relevance of such a regulation remain to be determined. In the present study, we have investigated cell genesis in the adult amygdala.

So far, only limited information has been obtained concerning the nature of the precursor cells in the brain parenchyma outside the "canonical" neurogenic regions of the adult brain, namely, the hippocampal dentate gyrus and the subventricular zone of the lateral ventricle (Arsenijevic et al. 2001; Palmer et al. 1995). The existence of parenchymal precursor cells (as "spongioblasts") was proposed by the early neuroanatomists such as His, Schaper, and later Penfield. The proteoglycan NG2 (neuron-glia 2; Wilson et al. 1981) identifies cells that show certain surprising characteristics intermediate between neuronal and glial properties (Butt et al. 2002; Stallcup

2002). For NG2 cells, the largely synonymous name "polydendrocytes" has been suggested (Nishiyama 2007), but as the alternative, "synantocyte" has not really been taken up by the community (Butt et al. 2005). A subset of NG2-expressing cells do indeed serve as oligodendrocyte progenitor cells in the mature central nervous system (CNS) and are capable of proliferating under physiological conditions and in response to CNS injury (Dawson et al. 2003; Di Bello et al. 1999; Horner et al. 2000; Levine and Nishiyama 1996; Reynolds et al. 2002), but many questions remain open. Since NG2-expressing cells are found in both gray and white matter with a similar distribution (Dawson et al. 2003), the differentiation potential of NG2-expressing cells has been proposed not to be restricted to the oligodendrocyte lineage, but also to extend to astrocytes (Zhu et al. 2008) and even neurons (Belachew et al. 2003). Whereas the potential for astrocytic differentiation had been predicted from work on classical O2A progenitor cells (Raff et al. 1983), which are thought to show an overlap with or even be identical to NG2 cells, the generation of new neurons has remained controversial. In any case, these findings need to be seen in the larger picture of possible roles that NG2 might play in plasticity (Sellers and Horner 2005). Some evidence indicates that NG2-expressing cells comprise a new class of glia capable of close interaction with neurons (Peters 2004). Synapses between neurons and NG2 cells undergo activity-dependent modifications analogous to long-term potentiation (LTP) at excitatory synapses (Ge et al. 2006). These findings make NG2 cells particularly interesting in the context of activity-dependent cellular plasticity.

Our previous work on adult hippocampal neurogenesis has stimulated our interest in the amygdala (or "amygdaloid complex", as it consists of numerous nuclei), because the amygdala is involved in processing the affective components of memory, most importantly fear and adverse reactions (Blair et al. 2001; Maren and Quirk 2004), in which the hippocampus and possibly adult hippocampal neurogenesis are also involved (Imayoshi et al. 2008; Revest et al. 2009). Whereas an extensive body of literature covers other aspects of amygdaloid plasticity with behavioral relevance (Maren 2005), little is known about the regulation of cell proliferation and differentiation in the amygdala in response to behavioral and environmental factors. The aim of the present study has thus been two-fold: (1) to extend the current knowledge of which types of cells are physiologically generated in the adult amygdala both by morphological criteria and by electrophysiology; (2) to determine whether two paradigms of physiological activity, namely, environmental enrichment and voluntary physical exercise, which are known for their neurogenic potential in the hippocampus (Brown et al. 2003), can regulate aspects of cell genesis in the adult amygdala.

Materials and methods

Animals, housing conditions, and bromodeoxyuridine injections

For experiments on the physiological regulation of cell genesis in the amygdala, female C57BL6/J mice (approximately 2 months of age at the beginning of the experiment) were obtained from Charles River (Sulzfeld, Germany). Animals were randomly assigned to one of three experimental conditions (enriched environment: ENR; physical activity: RUN; standard laboratory conditions: CTR). Animals undergoing environmental enrichment stayed in the ENR for 40 days and received one daily intraperitoneal injection of BrdU (5-bromo-2-deoxyuridine, Sigma; daily dose: 50 μg/g body weight) during the last 10 day of this period. In the ENR, 16 mice lived in a large cage (80×80 cm²) containing rearrangeable plastic tubes, nesting material, and mesh wire ladders. RUN mice were initially housed under standard conditions and were given *ad libitum* access to a running wheel (Tecniplast) for the last 10 days of the 40-day period, during which the animals also received daily BrdU injections. CTR mice were housed under standard laboratory conditions for the entire 40-day period, the last 10 days of which they received daily BrdU injections. For the detailed phenotypic analyses and the assessment of the long-term fate of BrdU-positive cells in the amygdala, we examined female C57BL6/J mice (approximately 3 months of age at the beginning of the experiment) that received 10 daily BrdU injections (50 μg/g body weight) and were killed at either 1 day, 4 weeks, 3 months, 6 months, or 1 year after the last BrdU injection; hippocampal data from this set of animals have been published independently (Kempermann et al. 2003). In order to examine the phenotypic nature of the cells in or close to division, co-labeling studies were performed with Ki-67, Phospho-Histone H3, and BrdU in animals that had been perfused 3 h after a single BrdU injection. The generation of the Nestin-green fluorescent protein (GFP) transgenic mice was as previously described (Yamaguchi et al. 2000). Local and federal regulations regarding animal welfare were followed.

Tissue preparation

Animals were killed with an overdose of ketamine and transcardially perfused with 0.9% NaCl solution followed by 4% paraformaldehyde in cold 0.1 M phosphate buffer (pH7.4). For postfixation, brains were kept in 4% paraformaldehyde at 4°C for 24 h and then transferred into 30% sucrose. Series of coronal sections (40 μm) were produced by using a dry-ice-cooled sliding microtome (Leica) and stored in cryoprotectant (25% ethylene glycol, 25% glycerine, and 0.05 M phosphate buffer) at –20°C. The sections were stained by using free-floating immunohisto-chemistry and prepared for BrdU detection by incubation in 2 N HCl for 30 min at 37°C and washes in 0.1 M borate buffer (pH 8.5) for 10 min.

Antibodies

All antibodies were diluted in TRIS-buffered saline (TBS; pH8.4) containing 0.1% Triton X-100 and 3% donkey serum (TBS-plus). Antibodies were tested with the appropriate negative controls (reciprocal omission of primary and secondary antibodies). In the present study, the following primary antibodies were used: rat anti-BrdU (Harlan Seralab) 1:500, rabbit anti-Ki67 (Novocastra) 1:500, mouse Phospho-Histone H3 (Cell Signaling Technology) 1:50, mouse anti-NeuN (anti-neuronal nuclei; Chemicon) 1:100, goat anti-Doublecortin (Santa Cruz Biotech) 1:200, mouse anti-PSA-NCAM (anti-poly-sialated neural cell adhesion molecule; Chemicon) 1:400, rabbit anti-NeuroD (Abcam) 1:200, rabbit anti-BLBP (anti-brain lipid-binding protein) 1:2000, rabbit anti-Olig2 (kind gift from J. Alberta) 1:1000, rabbit anti-S100β (Swant, Bellinzona, Switzerland) 1:2500, mouse anti-S100β (Chemicon) 1:1000, rabbit anti-NG2 (Chemicon) 1:200, goat anti-GFAP (anti-glial fibrillary acidic protein; Santa Cruz Biotech) 1:1000, mouse anti-CNPase (anti-2',3'-cyclic nucleotide 3'-phosphodiesterase; Abcam) 1:500, mouse anti-RIP (anti-receptor interacting protein; Developmental Studies Hybridoma Bank, University of Iowa) 1:200, rabbit anti-Iba-1 (anti-ionized calcium-binding adaptor molecule 1; Wako) 1:500, mouse anti-GFP (Chemicon) 1:500, rabbit anti-GFP (Abcam) 1:200, goat anti-GFP (Acris DPC-Biermann) 1:1000. Secondary antibodies, raised in donkey and conjugated with fluorescein isothiocya-nate, RhodaminX, or CY-5, were purchased from Jackson Laboratories (distributor: Dianova) and diluted 1:250 for immunohistochemistry.

Immunofluorescence

For immunofluorescence quantification of both BrdU-labeled cells and BrdU with phenotypic markers, we examined every sixth section throughout the entire right hemisphere. After pretreatment (see above) and a blocking step with TBS-plus, each section series was subjected to a primary antibody mixture and incubated for 48 h at 4°C. After washing the sections in TBS and TBS-plus, we exposed them to mixtures of secondary antibodies for 4 h at room temperature in the dark. Fluorescent sections were mounted in polyvinyl alcohol with diazabicyclo-octane as an antifading agent. Fluorescent signals were detected by using a spectral confocal microscope (Leica TCS SP2). All analyses were performed by using the sequential scanning

mode in order to avoid cross-bleeding between detection channels.

Quantification

Quantification of BrdU-positive cells in the amygdaloid complex was performed on double-stained sections for BrdU and NeuN by using a coronal section series that covered the entire rostro-occipital extent of the hemisphere (sections 240 μm apart). The amygdaloid complex was identified by anatomical criteria based on NeuN staining and following the Mouse Brain Library atlas (Rosen et al. 2000) available at http://www.mbl.org. As BrdU-positive cells in the amygdaloid complex were comparatively rare, the stereological procedure was modified to exclude the uppermost focal plane. To yield an estimate of the number of BrdU-positive cell numbers in the entire structure, the numbers counted were multiplied by 6. To yield the absolute number of BrdU-positive cells expressing a distinct antigenic phenotype, the relative proportion (%) of that phenotype was multiplied by the absolute number of BrdU-positive cells.

Preparation of acute brain slices for electrophysiology

Forebrain slices including the amygdala were acutely isolated from nestin-GFP transgenic mice of various ages (6-32 weeks) as described previously (Filippov et al. 2003). Slices for corpus callosum recordings were obtained from wild-type mice at postnatal day 6 (P6).

For acute brain slice preparation, mice were decapitated, and the brain was removed within 2 min and placed in ice-cold (4°C) bicarbonate-buffered salt solution, which was constantly equilibrated with carbogen (5% CO_2 and 95% O_2). This bath solution contained 134 mM NaCl, 2.5 mM KCl, 1.3 mM $MgCl_2$, 2 mM $CaCl_2$, 1.25 mM K_2HPO_4, 26 mM $NaHCO_3$, and 10 mM D-glucose, equilibrated with 95% O_2 and 5% CO_2 to a final pH of 7.4 The forebrain was dissected from the brainstem and was glued (cyanoacrylate glue) onto a glass block. The tissue was cut into 150-μm-thick coronal slices (in bicarbonate-buffered salt solution equilibrated with carbogen) by using a Leica VT1000S vibratome (Leica, Nussloch, Germany) and allowed to recover at room temperature. After a recovery period of 60 min, slices were gently placed onto a coverslip and fixed with a U-shaped platinum grid with nylon mesh in a recording chamber. The chamber was mounted on an upright microscope (Axiovert FS, Zeiss, Oberkochen, Germany) and was continuously perfused, at a flow rate of 4-6 ml/min, with carbogenated bath solution composed of 134 mM NaCl, 2.5 mM KCl, 1.3 mM $MgCl_2$, 2 mM $CaCl_2$, 1.25 mM K_2HPO_4, 26 mM $NaHCO3$, 10 mM D-glucose, bubbled with 95% O_2 and 5% CO_2 at a rate of 1-2 ml/min.

Electrophysiology

Membrane currents were measured with the patch-clamp technique in the whole cell voltage-clamp configuration (Hamill et al. 1981). Current signals were amplified with conventional electronics (EPC-9 amplifier, HEKA electronics, Lambrecht, Germany) filtered at 3 kHz and sampled at 5 kHz by an interface connected to an IBM compatible PC, which controlled the amplifier output. The acquisition and analysis of the data were performed with WinTIDA software (HEKA, Lambrecht/Pfalz, Germany). Capacitive currents and series resistance compensation (see below) were performed. Recording pipettes were produced from borosilicate glass capillaries (Hilgenberg, Malsfeld, Germany). Pipettes were filled with a salt solution that contained 130 mM KCl, 2 mM $MgCl_2$, 0.5 mM $CaCl_2$, 2 mM Na-ATP, 5 mM EGTA, and 10 mM HEPES. The pH was adjusted with KOH to 7.4. Pipette resistance was 4-8 MΩ. Series resistances were typically 16-33 MΩ, and series compensation was set to 80%. To obtain an estimate of the resting potential, we noted the membrane potential at the time of establishing the whole cell configuration.

To study the functional expression of AMPA (α-amino-3-hydroxy-5-methylisoxazole-4-proprionic acid)/kainate glutamate receptors in nestin-GFP-expressing cells in the amygdala and in the oligodendrocyte precursor cells in the corpus callosum, we tested the effect of kainate on membrane currents in the recorded cells. To minimize the indirect effects from neurons, 0.5 pM tetrodotoxin (TTX) and 0.1 mM $CdCl_2$ were added to the bath solution to block voltage-gated sodium and calcium channels, respectively. To examine glutamate transporter currents by applying D-aspartate, we added 5 pM TTX, 0.1 mM CdCl2, and 50 pM 6-cyano-7-nitro-quinoxaline-2,3-dione (CNQX; the AMPA/kainate glutamate subtype receptor blocker) to the bath solution in order to minimize interfering effects from neurons or by kainate/AMPA receptor activity.

Cellular identification

Cells located about 10-30 μm below the surface of the slice were visualized with water immersion optics by using a 510/20-nm band-pass filter for enhanced GFP fluorescence detection (excitation maximum: 490 nm) and photographed by using a charge-coupled device (CCD) camera (Watek Instruments) for recording cell size, location, and morphology. To label the recorded cells, Alexa Fluor 594 (10 μg/ml, Molecular Probes) was added to the pipette solution.

The amygdala was identified by standard transmission optics (Zeiss Axioskop, Zeiss; 5× Zeiss objective, numerical aperture: 0.15), and images were recorded with a CCD camera and stored on a computer (Variocam, PCO Computer Optics, Kelheim, Germany).

GFP-labeled cells were identified by fluorescence optics (excitation at 488 nm by using a monochromator; Polychrome IV, Till Photonics, Martinsried, Germany). The emitted light was collected at 530±10 nm with a CCD camera (QuantiCam Phase, Lübeck, Germany; 60× water immersion Olympus objective, numerical aperture: 0.8). After the patch clamp recording, Alexa Fluor 594 fluorescence was detected at an excitation wavelength of 589 nm and emission at 616±4 nm.

Statistical analysis

All statistical tests were chosen a priori and are described in detail in the main text.

Results

NG2 cells constitute the majority of proliferating cells in the adult amygdala

To examine the nature of proliferating cells in the adult amygdala, we labeled dividing cells with repeated injections of BrdU (once daily for 10 days) and studied the expression of various differentiation markers 1 day or 4 weeks after the last BrdU injection. Most BrdU-labeled cells were found to express NG2 at both time points (Fig. 1; 88.3±5.6% at 1 day and 79.6±2.4% at 4 weeks after BrdU; 1 day after BrdU: $n=5$ mice; 4 weeks after BrdU: $n=7$ mice; 50 BrdU-positive cells per mouse were analyzed for immunoreactivity against BrdU and NG2; data are presented throughout as mean±SEM). NG2/BrdU-positive cells typically had a kidney-shaped soma and extensively branched multipolar processes and were often located in the close vicinity of neurons (Fig. 2). The remaining BrdU-immunoreactive cells were CNPase-positive oligodendrocytes, Iba1-positive microglia, or S100β-positive/NG2-negative astrocytes (Fig. 2; for further details, see below).

No signs of neurogenesis in the amygdala of adult mice, but NG2 cells express a combination of neuronal and glial features

In order to characterize this cell population further, we performed immunocytochemical co-labeling studies. No BrdU-labeled cells in the amygdala were found to be immunoreactive for neuronal transcription factor NeuN (neither at 1 day nor at 4 weeks after BrdU injection; at each time point, we analyzed a total of 350 cells from seven animals for possible overlap of BrdU and NeuN immuno-reactivity), even at long time intervals after BrdU injection (3 months, 6 months, 1 year; at each time point, we analyzed a total of 40 cells from four animals for possible

overlap of BrdU and NeuN immunoreactivity). In agreement with previous reports (Deloulme et al. 2004), a large fraction of BrdU/NG2-positive cells expressed the calcium-binding protein S100β (Figs. 1, 2e, f; 95.6±3.1% at 1 day after BrdU and 74.2±6.7% at 4 weeks after BrdU). Only a few S100β/BrdU-positive cells did not co-express NG2 (3.8±2.2% at 1 day after BrdU and 6.1±1.0% at 4 weeks after BrdU; at each time point, we analyzed a total of 200 cells from four mice). The presence of NG2 ("neuron-glia 2") indicated an intermediate position between neuronal and glial properties. Accordingly, we found relatively homogeneous co-expression of several "glial" and some "neuronal" antigens in BrdU/NG2-positive cells. We detected the expression of neuronal microtubule-associated protein Doublecortin in a large fraction of BrdU/NG2-positive cells, both at 1 day and 4 weeks after BrdU (Fig. 2e, f). Generally, this immunoreactivity was weaker than in Doublecortin-positive cells in the neurogenic regions of the dentate gyrus or subventricular zone (Fig. 2g). The labeling was confined to an outer cytoplas-mic rim and proximal processes. Qualitative examination showed that most amygdala BrdU/NG2-positive cells were also weakly immunoreactive for neuronal transcription factor NeuroD, radial glia marker BLBP, transcription factor Olig2, vimentin, and Nestin (Fig. 2). In contrast, BrdU/NG2-positive cells were consistently devoid of GFAP, PSA-NCAM, NeuN, microglia marker Iba-1, and CNPase.

Next, we determined whether, during division, the cells in the amygdaloid complex exhibited similar immunocytochemical characteristics as the NG2-positive cell population identified in the BrdU study (which examined newly generated cells at the time-point of injection but did not reveal information about the proliferating population itself). Pulse-labeling of proliferating cells (with perfusion at 2 h after BrdU) and co-labeling studies by using cell-cycle associated markers (Ki-67 and Phospho-Histone H3) indicated that many cells in the cell cycle expressed NG2, S100β, and Doublecortin (Ki-67 + cells: 86.3±4.2% expressed NG2, 84.8±13.5% expressed Doublecortin, 65.9±3.3% expressed S100β; analysis of a minimum of 15 cells per mouse from seven mice; similar results were obtained with BrdU and Phospho-Histone H3; data not shown).

Few adult-generated amygdala cells show microglial and oligodendrocytic characteristics

To complete our immunocytochemical study of BrdU-labeled cells in the adult amygdala, we performed co-labeling studies with Iba1 (expressed in resting and activated microglia) and CNPase (expressed in myelinating oligodendrocytes). A small fraction of BrdU-positive cells in the amygdala was immunoreactive for Iba1 (Figs. 1, 2a; 8.12±2.89% at 1 day after BrdU, analysis of a total of 200
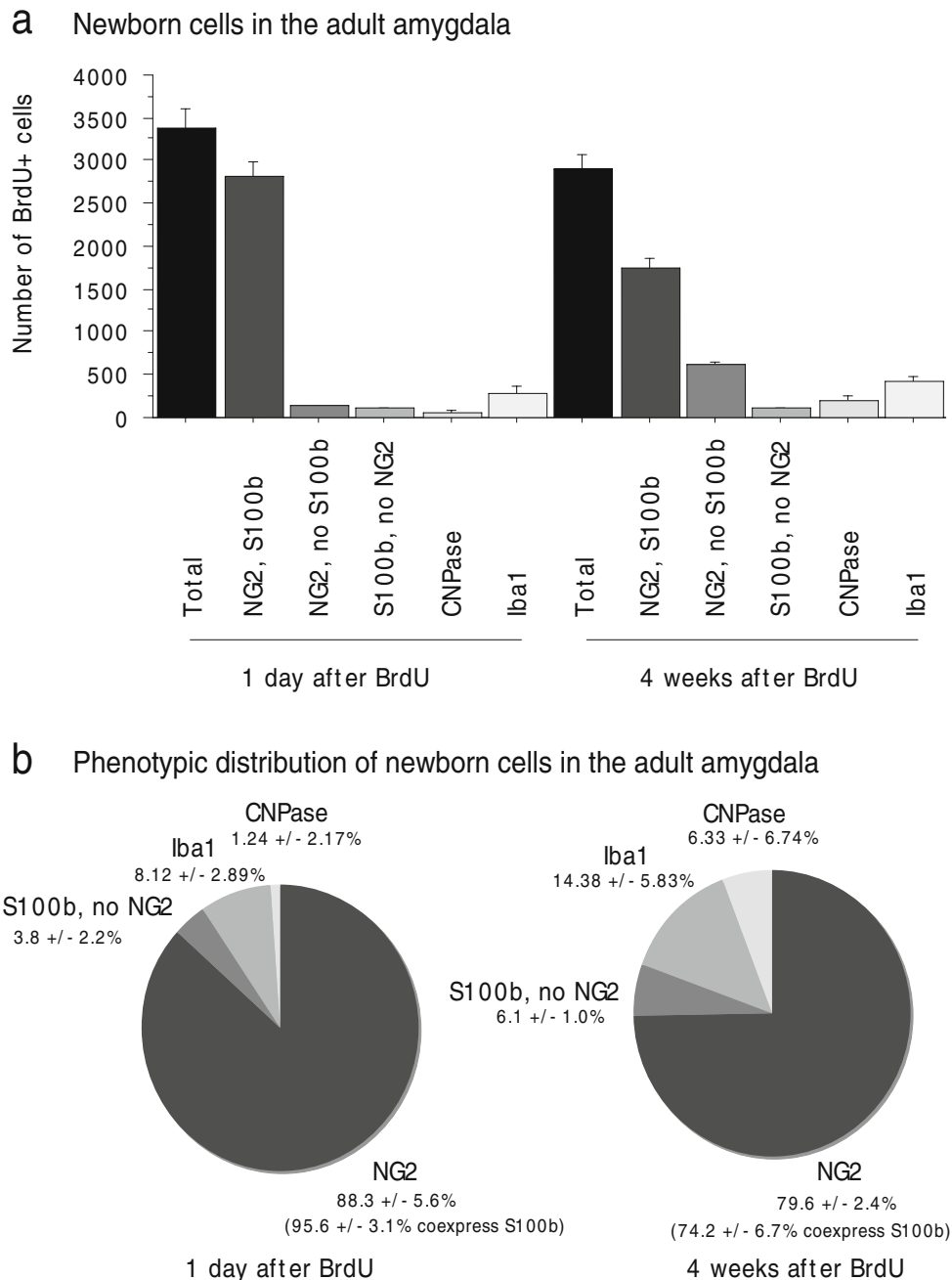
Fig. 1 Absolute (**a**) and relative (**b**) numbers of bromodeoxyuridine (BrdU)-positive cells and subpopulations at 1 day and 4 weeks after 10 BrdU injections. Most BrdU-positive cells were neuron-glia 2 (NG2)-immunoreactive and weakly co-expressed S100β (*S100b*). These cells appeared to proliferate slowly, and many of them still expressed NG2 at 4 weeks after BrdU. Microglia (expressing ionized calcium-binding adaptor molecule 1 [Iba-1]) and oligodendrocytes (expressing 2',3'-cyclic nucleotide 3'-phosphodiesterase [CNPase]) constituted smaller fractions of the total BrdU-positive cells (*error bars* SEM)

BrdU-positive cells from four animals; 14.38±5.83% at 4 weeks after BrdU, analysis of a total of 300 BrdU-positive cells from six animals). These cells were frequently encountered in the neuropil and in the medial and cortical nuclei of the amygdala, but rarely in the basolateral complex. The oligodendroglial marker CNPase was expressed by a small percentage of BrdU-positive cells (Figs. 1, 2d; 1.24±2.17% of all BrdU-positive cells at 1 day after BrdU, analysis of a total of 300 BrdU-positive cells from six animals; 6.33±6.74% of all BrdU-positive cells at 4 weeks after BrdU, analysis of a total of 350 BrdU-positive cells from seven animals).

NG2 progenitor cells give rise to oligodendrocytes and astrocytes in vivo (Zhu et al. 2008). Even though the present study of NG2 cells in the amygdala was not specifically designed to determine lineage relationships, our data are consistent with a slow transition of a subset of NG2 cells into oligodendrocytes. We detected a significant reduction in the number of BrdU/NG2-positive cells over the 4-week time period (2960±149.5 cells at 1 day after BrdU, analysis of a total of 200 BrdU-positive cells from four animals; 2356±150.8 cells at 4 weeks after BrdU, analysis of a total of 350 BrdU-positive cells from seven animals; t-test: $P=0.0281$). No significant difference was observed in the number of BrdU/CNPase-positive cells between time points, although the mean of the distributions clearly increased from 1 day to 4 weeks after BrdU (53±34 BrdU/CNPase-positive cells at 1 day after BrdU, analysis of a total of 300 BrdU-positive cells from six animals; 185 ±76.4 BrdU/CNPase-positive cells at 4 weeks after BrdU, analysis of a total of 350 BrdU-positive cells from seven animals; t-test: $P=0.1658$). In a parallel study, we examined phenotypic features of BrdU-positive cells up to 1 year after multiple BrdU injections (1 daily injection over 10 consecutive days). Six months after BrdU, 21 out of 40 cells (total from four animals) expressed CNPase, but not NG2. Taken together, these data are consistent with the notion that a subset of proliferating amygdala NG2 cells slowly differentiates into CNPase-positive myelinating oligodendrocytes, but certainly the majority of BrdU/ NG2-positive remain NG2-positive over the time period of 4 weeks after cell division (see also Discussion).

NG2 cells in the amygdala have electrophysiological properties of oligodendrocyte precursor cells

Next, we wanted to characterize the electrophysiological properties of amygdala NG2 precursor cells. As no NG2 reporter mouse was available at the time that these experiments were performed, we chose an indirect approach. Considerable cellular overlap of Nestin and NG2 expression occurs in the amygdala, and accordingly, Nestin-GFP reporter mice represent a reasonable tool for cellular investigations of a subset of amygdala NG2 progenitors. In Nestin-GFP reporter mice (Yamaguchi et al. 2000), we first determined the overlap of NG2 and Nestin-GFP immunoreactivity and found all GFP-positive cells in the amygdala to be NG2-positive, whereas 44.4±7.8% of amygdala NG2 cells showed Nestin-GFP expression (a total of 150 cells from three animals was analyzed). These observations confirmed that Nestin-GFP labeled a subset of amygdala NG2 cells.

We subsequently tested for the expression of voltage-gated channels, AMPA/kainate receptors, and glutamate transporters in Nestin-GFP-positive cells in the adult amygdala (Fig. 4). Nestin-GFP cells could be recognized by their green fluorescence and could thus be approached with a patch pipette. To reveal the morphological features of the recorded cell, the hydrophilic fluorescent dye Alexa Fluor 594 (10 μg/ml) was added to the pipette solution, and the cell was brightly stained after dialysis (Fig. 3a). Once the whole cell recording configuration had been established in the voltage clamp mode (Hamill et al. 1981), membrane currents were activated by clamping the membrane at a holding potential of -70 mV to hyper- and depolarizing potentials ranging from -180 to +80 mV (50 ms, 10-mV increments). We selected cells with a stable membrane potential between -50 and -85 mV ($n=51$ cells).

Three different patterns of membrane currents were distinguishable. The majority of Nestin-GFP-expressing cells (27 out of 51 cells) expressed outwardly rectifying currents activated with depolarization and inwardly rectifying inactivation currents with hyperpolarization (Fig. 3a). The current voltage curve revealed a reversal potential close to the K^+ equilibrium potential (Fig. 3a). A second population of cells (19 out of 51 cells) displayed a current pattern characterized by the presence of outwardly rectifying currents with depolarization and voltage- and time-independent currents with hyperpolarization (Fig. 3a). The current voltage curve revealed outwardly rectifying properties and a reversal potential close to the K^+ equilibrium potential (Fig. 3a). Few cells (three out of 51 cells) had neuronal properties. Rapidly activating and inactivating inward currents were trigged with depolarization positive to about −50 mV typical for voltage-gated Na^+ currents (Fig. 3a). The inward current was followed by an outward current with a reversal potential close to the K^+ equilibrium potential (Fig. 3a). Action potentials could be recorded after depolarizing current injection in the current clamp mode and displayed the depolarizing current-dependent frequency (Fig. 3b). We also observed spontaneous synaptic activity in the three cells (Fig. 3b). The rise time of these spontaneous currents was about 1.5 ms, and the decay time constant (as determined by monoexponential fitting) ranged between 7 and 105 ms ($n=3$), with peak amplitudes ranging from 39 to 154 pA. The spontaneous activity could be blocked by bicuculline ($n=3$; 20 μM) indicating that precursor cells receive neuronal gamma-aminobutyric-acid (GABA)-ergic input (Fig. 3b).

The expression pattern of glutamate receptors and transporters distinguishes neurogenic astrocyte-like precursor cells in the dentate gyrus from non-neurogenic astrocytes in hippocampal area CA1. Whereas astrocyte-like precursor cells in the dentate gyrus (type-1 cells; Filippov et al. 2003) express glutamate receptors and transporters, CA1 astrocytes express either receptors or transporters. To characterize the functional expression pattern of glutamate receptors/transporters in amygdala precursor cells, we recorded electrophysiological responses
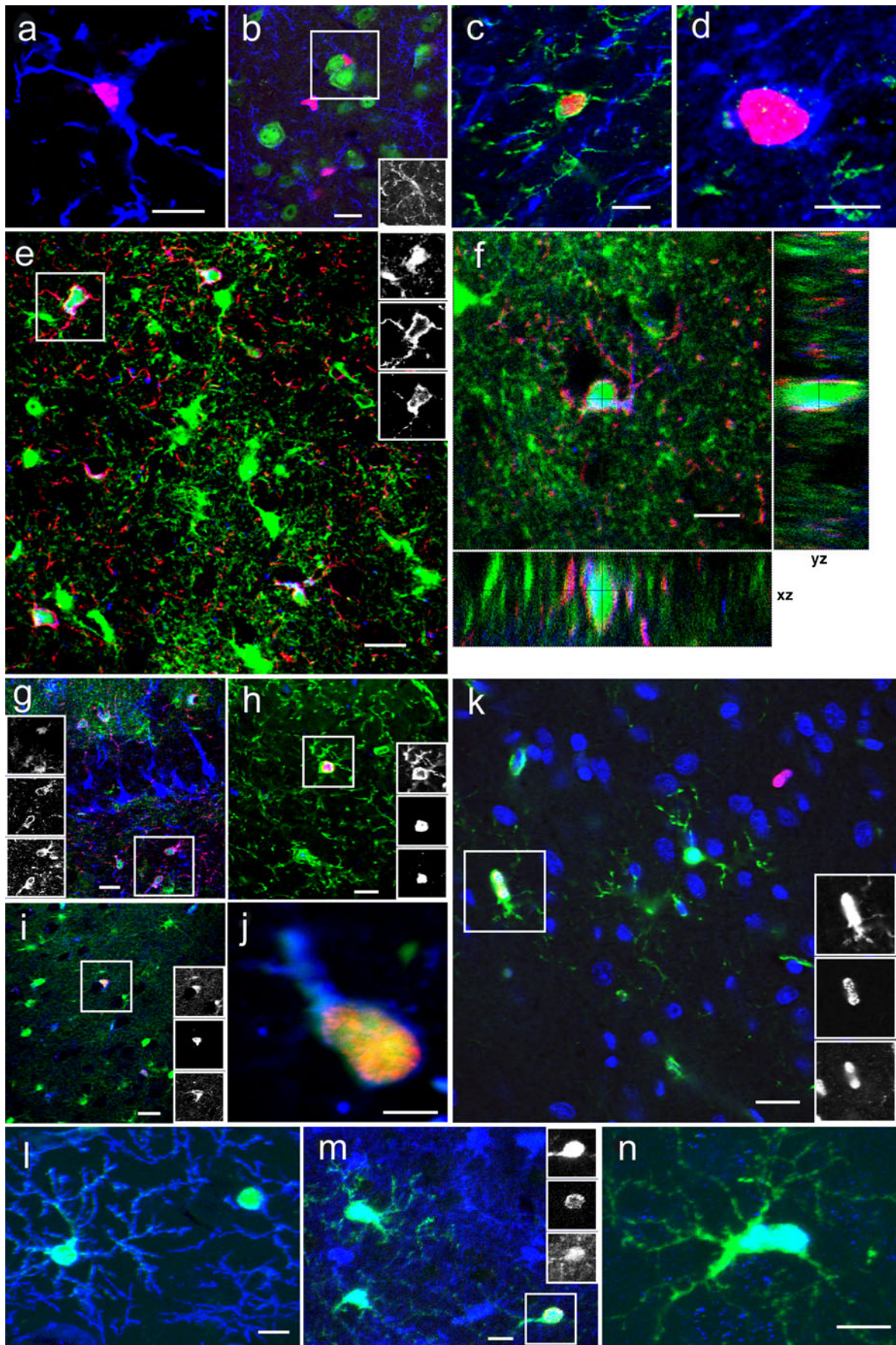
◄ **Fig. 2** Phenotypic analyses of BrdU-positive cells in adult amygdala.
a Iba1-positive (*blue*) ramified microglial cell with incorporated BrdU
(*red*). *Bar* 10 μm. **b** Many BrdU-positive (*red*) cells that expressed
NG2 (*blue*, *box*) were found close to neuronal cell bodies, as identified
by immunoreaction for the neuronal transcription factor NeuN (*green*).
Bar 20 μm. **c** No overlap of immunoreactivity for proteoglycan NG2
(*green*) and oligodendroglial marker CNPase (*blue*) in BrdU-positive
(*red*) cells. *Bar* 7.5 μm. **d** At 1 day and 4 weeks after BrdU, few
newborn (*red* BrdU) cells in the adult amygdala showed oligoden-
droglial characteristics (*blue* CNPase). *Bar* 7.5 μm. **e** One example
(*boxed*) of many NG2-positive (*red*, *middle box*) cells also expressing
S100β (*green*, *upper box*). In addition, weak immunoreactivity was
often noted for Doublecortin (*blue*, *lower box*). *Bar* 10 μm. **f** Z-stack
of confocal images (1 μm apart) through an NG2-positive (*red*) cell
demonstrating that Doublecortin (*blue*) and S100β (*green*) immuno-
reactivity are localized to the same cell. *Bar* 10 μm. **g** An example
(*boxed*) of NG2-positive (*red*, *middle box*) cells co-expressing
Doublecortin (*blue*, *lower box*) and S100β (*green*, *upper box*) in the
hilus of the dentate gyrus. In contrast to the Doublecortin-positive
cells in the subgranular zone and granule cell layer, these cells showed
weak immunoreactivity for Doublecortin, which was confined to a
cytoplasmic rim and proximal processes. *Bar* 20 μm. **h** BrdU-positive
(*red*, *middle box*) cell (*boxed*) in the amygdala expressing NG2 (*green*,
upper box) and Vimentin (*blue*, *lower box*). *Bar* 15 μm. **i** The *boxed*
perineuronal satellite cell expressed BrdU (*red*, *middle box*), S100β
(*green*, *upper box*), and Doublecortin (*blue*, *lower box*). *Bar* 25 μm. **j**
Nestin-green fluorescent protein (GFP; *green*) cell immunoreactive for
BrdU (*red*) and Doublecortin (*blue*). *Bar* 5 μm. **k** Nestin-GFP (*green*,
upper box) cell immunoreactive for NeuroD (*blue*, *lower box*) and
BrdU (*red*, *middle box*). *Bar* 20 μm. **l** Subpopulation of NG2-positive
cells (*blue*) expressing Nestin-GFP (*green*). *Bar* 10 μm. **m** An example
(*boxed*) of newborn (BrdU; *red*, *middle box*) cells also found to
express BLBP (brain lipid-binding protein; *blue*, *lower box*) in the
amygdala. In addition, this cell exhibited Nestin-GFP expression
(*green*, *upper box*). *Bar* 7.5 μm. **n** This Nestin-GFP (*green*) cell was
immunoreactive for transcription factor Olig2 (*blue*). *Bar* 7.5 μm

of amygdala Nestin-GFP-expressing cells to kainate or D-
aspartate application. Bath application of kainate (0.5 mM,
30 s) triggered an inward current in all measured cells
($n=29$ cells) while clamping the membrane at –70 mV
(Fig. 4a, b). To determine the reversal potential of the
kainate response, the membrane was clamped to a series of
de- and hyperpolarizing potentials ranging from –130 to
90 mV from a holding potential of –70 mV with 20-mV
increments. These series of voltage jumps were repetitively
applied and allowed us to study the conductance changes
over time and to construct I/V curves in 6-s intervals.
Kainate evoked a complex response, which was composed
of three different components (Fig. 4a). Within a few
seconds after application, the resting K^+ conductance
decreased, and the reversal potential of this blocked
conductance was at 0 mV. Both the inward and the outward
K^+ conductance were affected. Subsequently, a conductance
increase developed that had a reversal potential of 0 mV
indicating that a cationic current was activated. This
conductance increase returned to baseline within about
4 min after washout of kainate. With a delay of 3–4 min
after washout of kainate, an outwardly rectifying current

developed with a reversal potential of -70 mV. This outward
K^+ conductance returned to baseline after about 5 min. The
resting K^+ conductance, which was reduced in amplitude at
the beginning of the response, remained reduced, even after
20 min of recording time. In conclusion, kainate triggered a
rapid and long-lasting blockade of the resting K^+ conduc-
tance, a transient cationic current, and with a significant
delay, a transient increase of an outwardly directed K^+
conductance. Some heterogeneity occurred with respect to
the late-developing K^+ outward conductance: it was not
found in nine out of 29 cells (Fig. 4b). The presence of
glutamate transporter currents was examined by assessing
currents after the application of D-aspartate (D-aspartate is
a glutamate transporter substrate but not a ligand for
glutamate receptors). No currents were recorded after D-
aspartate application ($n=20$ cells; Fig. 4c). Thus, we
conclude that amygdala Nestin-GFP-positive cells express
functional glutamate receptors of the AMPA/kainate sub-
type, but no glutamate transporters, a profile that differs
from neurogenic astrocyte-like precursor cells in the dentate
gyrus (Filippov et al. 2003).

To compare the electrophysiological properties of
Nestin-GFP-positive cells in the amygdala with those of
oligodendrocyte precursor cells, we analyzed cells in the
corpus callosum in P6 brain slices. Oligodendrocyte
progenitor cells have membrane currents distinct from
mature oligodendrocytes (Berger et al. 1991). Membrane
currents were recorded by using the paradigm described
above. Consistent with previous reports (Sontheimer et al.
1989), oligodendrocyte progenitor cells expressed outwardly
rectifying currents activated by depolarization (Fig. 5a). We
then tested for the functional expression of glutamate
receptors and glutamate transporters by using the protocol
described above. At a membrane potential of –70 mV, bath
application of kainate (0.5 mM, 30 s) triggered an inward
current in all recorded cells ($n=10$ cells). In seven out the 10
cells, kainate evoked a complex response as observed in
amygdala cells; this was composed of three different
components, namely the activation of a cationic conduc-
tance, blockade of the resting K^+ conductance, and activation
of a transient K^+ conductance (Fig. 5c). In the remaining
cells, the first two components were observed, whereas
the transient K^+ outward conductance was not recorded.
To test for the presence of functional glutamate trans-
porters, we applied D-aspartate. In none of the cells did
we observe any current response ($n=10$; Fig. 5b). Thus, we
conclude that oligodendrocyte progenitor cells in the corpus
callosum express functional glutamate receptors of the
AMPA/kainate subtype, but no glutamate transporters. Taken
together, these data indicate that amygdala Nestin-GFP-
positive precursor cells have similar electrophysiological
characteristics as oligodendrocyte progenitors from the corpus
callosum.
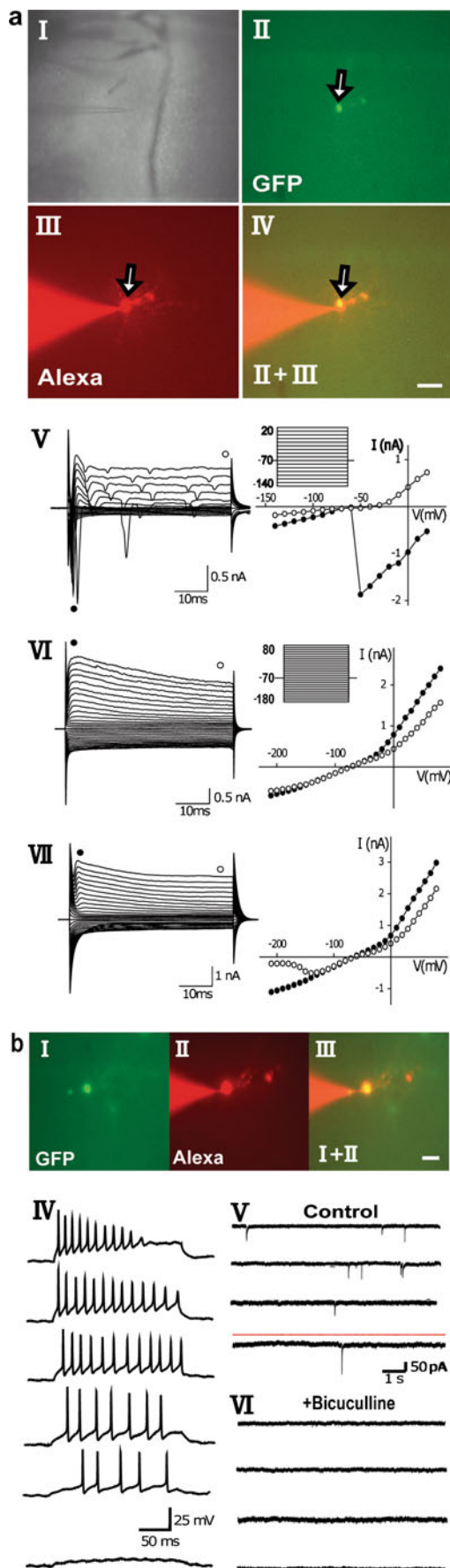
◀ **Fig. 3** Electrophysiological properties of Nestin-GFP expressing cells in adult amygdala. **a** Morphology and current pattern of Nestin-GFP-expressing cells in the amygdala from adult Nestin-promoter-GFP transgenic mice. *I* Bright-field image of an amygdala slice showing the position of the patch pipette during recording. *II* Fluorescence image of GFP-expressing cells. *III* After recording, the cell (*arrow*) was dialyzed with Alexa Fluoro 594 via the pipette solution. *IV* Merged image verifying that GFP and Alexa Fluoro 594 labels correspond. *Bar* 120 μm (*I*), 15 μm (*II–IV*). *V, left* Membrane currents were evoked in the shown cell by applying 50-ms voltage steps ranging from –140 mV to +20 mV from a holding potential of –70 mV (for the recording protocol, see *inset*). Note the transient inward current. *V, right* Voltage curve obtained from data shown *left*; current amplitudes at the beginning (*black circles*) and at the end (*open circles*) of the voltage pulse were plotted against the holding potential. *VI, left* Membrane currents from the shown cell were evoked by 50-ms voltage steps ranging from –210 mV to +80 mV from a holding potential of –70 mV (for the recording protocol, see *inset*). *VI, right* Outwardly rectifying current to voltage curve was obtained from data shown *left*; current amplitudes at the beginning (*black circles*) and at the end (*open circles*) of the voltage pulse were plotted against the holding potential. *VII* As described in *VI*, another GFP-positive cell was characterized by an outwardly rectifying and inwardly rectifying current voltage curve. **b** Neuronal properties were observed in a few Nestin-GFP-expressing cells in the amygdala. *I-III* Fluorescence images of a GFP-expressing cell in the amygdala; this cell displays the sodium currents shown in *V*; (*I*) GFP, (*II*) Alexa Fluoro 594, (*III*) merged. *Bar* 25 μm. *IV* In the current clamp mode, action potentials could be recorded after the depolarizing current injection (note the depolarizing current-dependent frequency). *V, VI* Spontaneous activity was recorded under control conditions (*V*) or in the presence of bicuculline (20 μM, *VI*)

Environmental enrichment and physical activity lead to a reduction in microgliogenesis and an increase in BrdU/NG2 cells lacking S100β

We next wanted to test whether the proliferation and/or differentiation of amygdala NG2 precursor cells is/are regulated by behavioral or environmental factors, as is the case for precursor cell populations in other parts of the brain (Kempermann et al. 1997; van Praag et al. 1999). C57BL/6J mice were housed under either standard laboratory conditions (CTR), in an ENR, or had access to a running wheel in their home cage (RUN), as previously described (Ehninger and Kempermann 2003). BrdU was injected once daily during the last 10 days of the experiment. Half of the animals were killed 1 day later, and the remaining mice were killed 4 weeks after the last injection. Stereological cell counting of BrdU-positive nuclei in the dentate gyrus served as an internal control and allowed the replication of the previous findings (Kempermann et al. 1997; van Praag et al. 1999) in the present study (Fig. 6a). Both stimuli increased neurogenesis in the dentate gyrus.
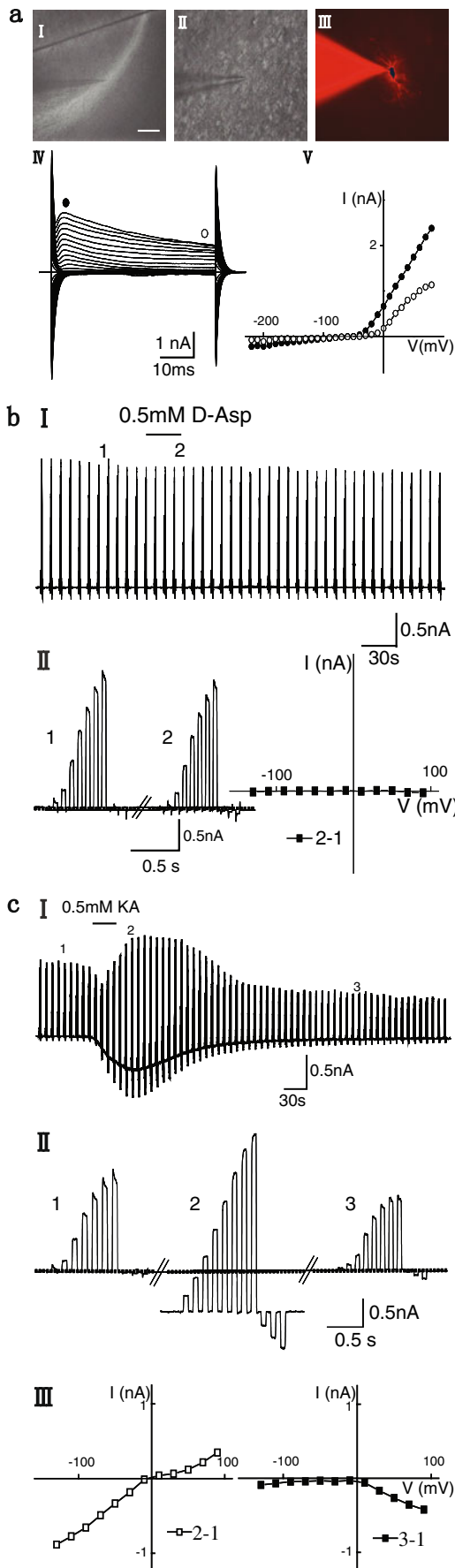
The counting of BrdU-positive cells in the amygdala revealed no statistically significant difference between the experimental groups at 1 day after BrdU (Fig. 6b; one-way
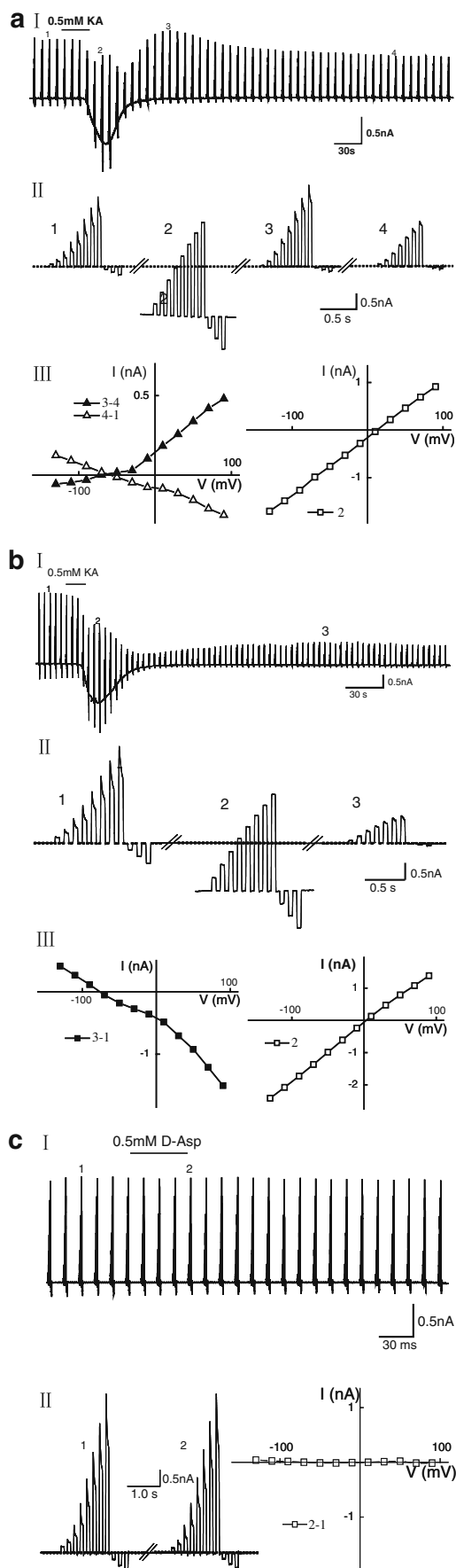
◀ **Fig. 4** **a** Functional expression of AMPA/kainate glutamate receptors in Nestin-GFP-expressing cells in the amygdala. *I* During recording of membrane currents from a Nestin-GFP-expressing cell, kainate (*KA*, 0.5 mM, 30 s) was applied as indicated. The membrane was clamped from a holding potential of -70 mV to a series of de- and hyperpolarizing potentials ranging between -130 mV to +90 mV with 20-mV increments. At this time resolution, the single voltage steps cannot be resolved. *II* Four series of voltage steps from the recording shown in *I* taken before (*1*) and at the peak (*2*) of the kainate response and revealing the developed outward rectifying current (*3*) and the long-term blockage of the resting K⁺ conductance (*4*), but shown with higher time resolution (these traces were used to construct a current voltage curve, as shown in *III*, *left*). *III*, *left* Current voltage curves of long-term blockage of the resting K⁺ conductance were obtained by subtracting current amplitudes at the corresponding membrane potentials before and about 12 min after the kainate application (*4-1*). The reversal potential was close to -80 mV. The current voltage curves of the outward rectifying current were obtained by subtracting current amplitudes at the corresponding membrane potentials at the peak of the outward rectifying current and about 12 min after the kainate application (*3-4*). The reversal potential was close to -70 mV. *III*, *right* Current voltage curves of kainate-triggered responses were obtained by current amplitudes at the corresponding membrane potentials at the peak response during the kainate application (*2*). The reversal potential was at 0 mV. **b** Another profile of the kainate-evoked response current in Nestin-GFP-expressing cells in the amygdala. *I* As in **a**, kainate (0.5 mM, 30 s) was applied while recording membrane currents from a GFP-expressing cell that displayed a different kainate-triggered response profile over time (10 out of 21). *II* Three series of voltage steps from the recording shown in *I* taken before (*1*) and at the peak (*2*) of the kainate response and during long-term blockage of the resting K⁺ conductance (*3*), but shown with higher time resolution (these traces were used to construct a current voltage curve as shown in *III*). *III*, *left* Current voltage curves of long-term blockage of the resting K⁺ conductance were obtained by subtracting current amplitudes at the corresponding membrane potentials before and about 12 min after the kainate application (*3-1*). The reversal potential was close to -80 mV. *III*, *right* Current voltage curves of kainate-triggered responses were obtained by current amplitudes at the corresponding membrane potentials at the peak response during the kainate application (*2*). The reversal potential was at 0 mV. **c** Nestin-GFP-expressing cells in the amygdala lacked glutamate transporter currents. *I* No current response to D-aspartate (*D-Asp*) application (0.5 mM, 30 s) to nestin-GFP-expressing cells (*n*=10 out of 10). *II*, *left* Two series of voltage steps from the recording shown in *I* taken before (*1*) and during the D-aspartate application (*2*). *II*, *right* Current voltage curve; no current was induced by the D-aspartate application

analysis of variance [ANOVA]: $F_{(2,18)}=0.15$; $P=0.8618$; ENR: $n=7$ mice, RUN: $n=7$ mice; CTR: $n=7$ mice) but a significant reduction in the ENR and RUN groups as compared with controls at 4 weeks after BrdU (Fig. 6b; one-way ANOVA: $F_{(2,20)}=6.236$; $P=0.0079$; Fisher's post hoc test: ENR vs. CTR: $P=0.0143$; RUN vs. CTR: $P=0.0035$; RUN vs. ENR: $P=0.4827$; ENR: $n=8$ mice, RUN: $n=7$ mice; CTR: $n=8$ mice).

We next performed co-labeling studies to determine which cell population(s) accounted for these group differences. The number of BrdU-positive microglia (co-expressing Iba-1) was significantly reduced in RUN and ENR as compared with CTR at 4 weeks after BrdU (Fig. 6e; one-

◀ **Fig. 5 a** Current features of putative oligodendrocyte precursor cells in the mouse corpus callosum. **a** *I* Bright-field image of a corpus callosum slice showing the location of the cell. *II* Bright-field image at high magnification of the patched cell during recording. *III* Fluorescence image of the recorded cell dialyzed with Alexa Fluro 594 via the pipette solution. *Bar* 120 μm (*I*), 15 μm (*II*, *III*). *IV* Membrane currents from the cell shown were evoked by 50-ms voltage steps ranging from –210 mV to +80 mV from a holding potential of –70 mV (for the recording protocol, see *inset* in *V*). *V* Outwardly rectifying current to voltage curve was obtained from *IV*; current amplitudes at the beginning (*black circles*) and at the end (*open circles*) of the voltage pulse were plotted against the holding potential. **b** Putative oligodendrocyte progenitor cells in the corpus callosum lack glutamate transporter current expression. *I* As described in Fig. 4a, no current response to D-aspartate (*D-Asp*) application (0.5 mM, 30 s) was recorded in a putative oligodendrocyte progenitor cell (*n*=10 out of 10). *II, left* Two series of voltage steps from the recording shown in *I* taken (*1*) before and (*2*) during the D-aspartate application. Current voltage curve: no current was recorded after the D-aspartate application. **c** Functional expression of AMPA/kainate glutamate receptors in the putative oligodendrocyte precursor cells in the corpus callosum. *I* As described in Fig. 4a, kainate (*KA*, 0.5 mM, 30 s) was applied while membrane currents were recorded (*n*=7 out of 10). *II* Three series of voltage steps from the recording shown in *I* taken (*1*) at the peak of the kainate response, (*2*) after long-term blockage of the resting K$^+$ conductance, and (*3*) with higher time resolution. *III, left* Current voltage curves of kainate-triggered responses were obtained by subtracting current amplitudes at the corresponding membrane potentials before and at the peak response during the kainate application (*2-1*). The reversal potential was at 0 mV. *III, right* The current voltage curves of long term blockage of the resting K+ conductance were obtained by subtracting current amplitudes at the corresponding membrane potentials before and about 12 min after the kainate application (*3-1*)

way ANOVA: $F_{(2,15)}=4.268$; $P=0.0341$; Fisher's post hoc test: ENR vs. CTR: $P=0.0364$; RUN vs. CTR: $P=0.0163$; ENR: *n*=7 mice; RUN: *n*=6 mice; CTR: *n*=5 mice). Additionally, co-labeling for BrdU and S100β revealed a significant reduction of BrdU/S100β cells in the ENR and RUN groups relative to controls at 4 weeks after BrdU (Fig. 6d; one-way ANOVA: $F_{(2,18)}=13.111$; $P=0.0003$; Fisher's post hoc test: ENR vs. CTR: $P=0.0001$; RUN vs. CTR: $P=0.0028$; ENR: *n*=6 mice; RUN: *n*=7 mice; CTR: *n*=8 mice). In contrast, co-labeling studies for NG2 and

Fig. 6 Regulation of cell proliferation and differentiation in the adult ▶ amygdala by environmental enrichment (*ENR*) and physical activity (*RUN*). **a** Consistent with previous findings, RUN and ENR increased the number of BrdU-positive cells in the dentate gyrus relative to controls (*CTR*). **b** In the amygdala, ENR and RUN did not change the number of BrdU-positive cells at 1 day (*1 d*) after BrdU as compared with CTR. At 4 weeks (*4 w*), however, significantly fewer BrdU-positive cells were counted in ENR and RUN than in CTR. **c** The number of BrdU-positive cells expressing NG2 did not significantly differ between experimental groups. **d, e** A marked reduction, however, in the number of BrdU/S100β-positive cells (**d**) and BrdU/Iba1-positive cells (new microglia; **e**) was noted at 4 weeks after BrdU. **f** The number of newborn oligodendrocytes (CNPase-positive) was not measurably affected by ENR and RUN. **g, h** The apparent loss of BrdU/S100β cells in ENR and RUN was caused by an increase in the number (**g**) and proportion (**h**) of BrdU/NG2 cells that did not express S100β (*error bars* SEM). *$P<0.05$, **$P<0.01$
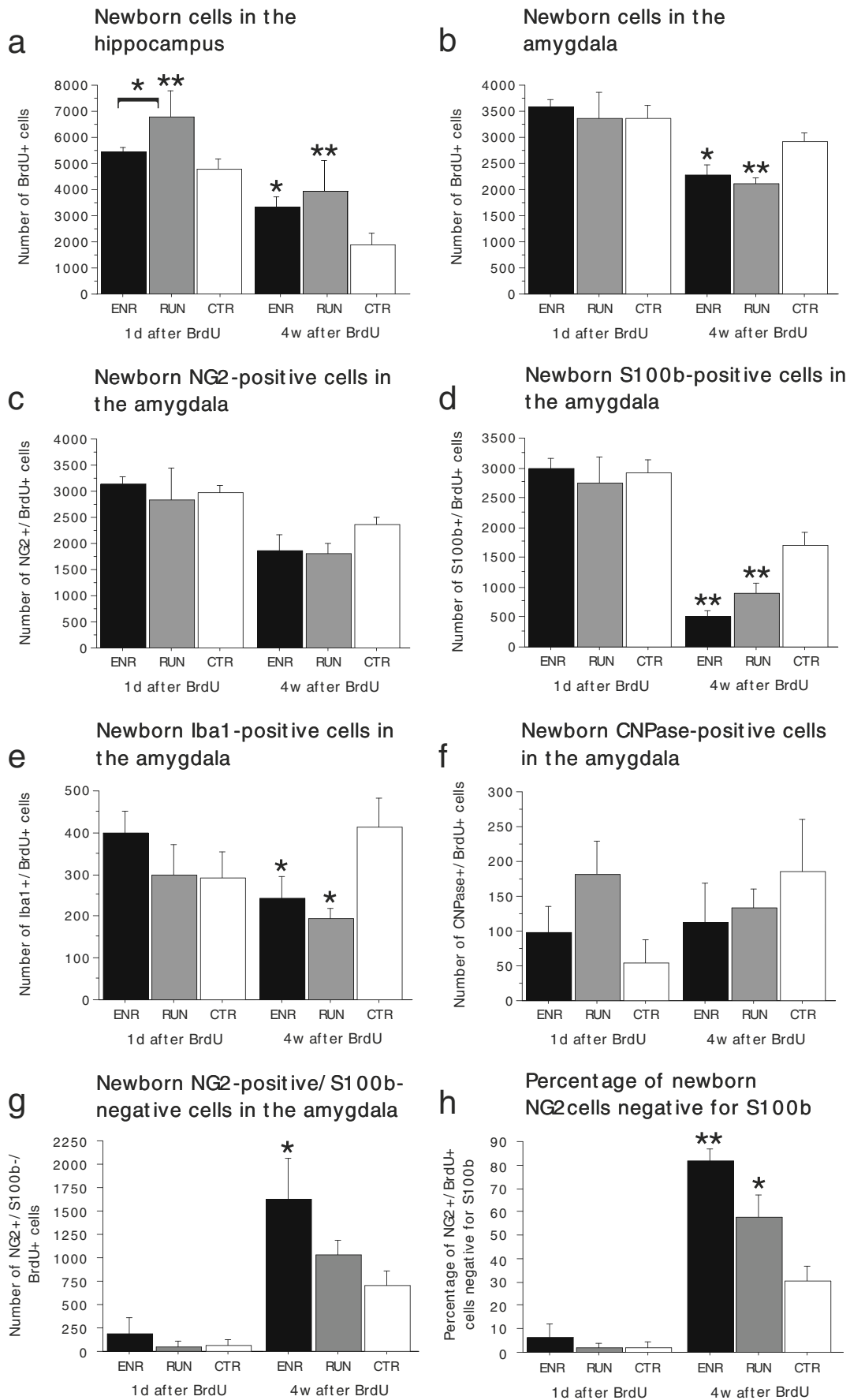
BrdU suggested that the number of NG2/BrdU-positive cells was unaltered in ENR and RUN (Fig. 6c; one-way ANOVA: F(2,13)=2.603; P=0.1120; ENR: n=4 mice; RUN: n=5 mice; CTR: n=7 mice). As the vast majority of BrdU/S100β cells also expressed NG2, these observations suggest that RUN and ENR caused a strong increase in the proportion of S100β-negative NG2/BrdU double-positive cells at 4 weeks after BrdU. Accordingly, we next determined the number and proportion of S100β-negative NG2/BrdU double-positive cells in the amygdala. We found a significant increase of this population in ENR and RUN at 4 weeks after BrdU (Fig. 6g, h; number: one-way ANOVA: F(2,12)=4.112; P=0.0436; Fisher's post hoc test: ENR vs. CTR: P=0.0144; RUN vs. CTR: P=0.2509; proportion: one-way ANOVA: F(2,12)=10.060; P=0.0027; Fisher's post hoc test: ENR vs. CTR: P=0.0010; RUN vs. CTR: P=0.0194; ENR: n=3 mice; RUN: n=5 mice; CTR: n=7 mice). The number of CNPase/BrdU-positive cells was not measurably affected by either experimental intervention (Fig. 4f; one-way ANOVA: F(2,17)=0.407; P=0.6722; ENR: n=7 mice; RUN: n=6 mice; CTR: n=7 mice). In summary, these findings demonstrate that ENR and RUN lead to a reduced formation of new microglia and suggest that ENR and RUN cause a loss of S100β expression in BrdU/NG2 cells in the adult amygdala.

Environmental enrichment and physical activity might also lead to an increase of BrdU/NG2 cells lacking S100β in layer II/III of the visual cortex

Our next objective was to determine whether ENR and RUN induce a loss of S100β expression in BrdU/NG2 cells specifically in the amygdala, or if this is a more widespread phenomenon. ENR has effects on various brain areas, but many studies have highlighted structural changes in the visual cortex (Bennett et al. 1964; Diamond et al. 1964; Greenough and Volkmar 1973; Sirevaag and Greenough 1985, 1991; Szeligo and Leblond 1977; Turner and Greenough 1985; Walsh 1981). Increases in the thickness of the visual cortex as a response to ENR appear to be largely attributable to changes in layer II/III (Diamond et al. 1964). Cortical layers II/III contain elaborate horizontal intra-cortical connections that undergo activity- and experience-dependent modifications (Rioult-Pedotti et al. 1998). Accordingly, we determined whether ENR-triggered plastic changes in layer II/III of the visual cortex were accompanied by alterations in the resident population of newborn NG2-positive/S100β-negative cells. To this end, we counted the total number of BrdU-positive cells in layers II/III of the visual cortex of ENR, RUN, and CTR animals and examined the co-labeling of BrdU with either S100β or NG2 in a sample of cells (50 cells were analyzed per animal; triple-labeling for BrdU, S100β, and NG2 was
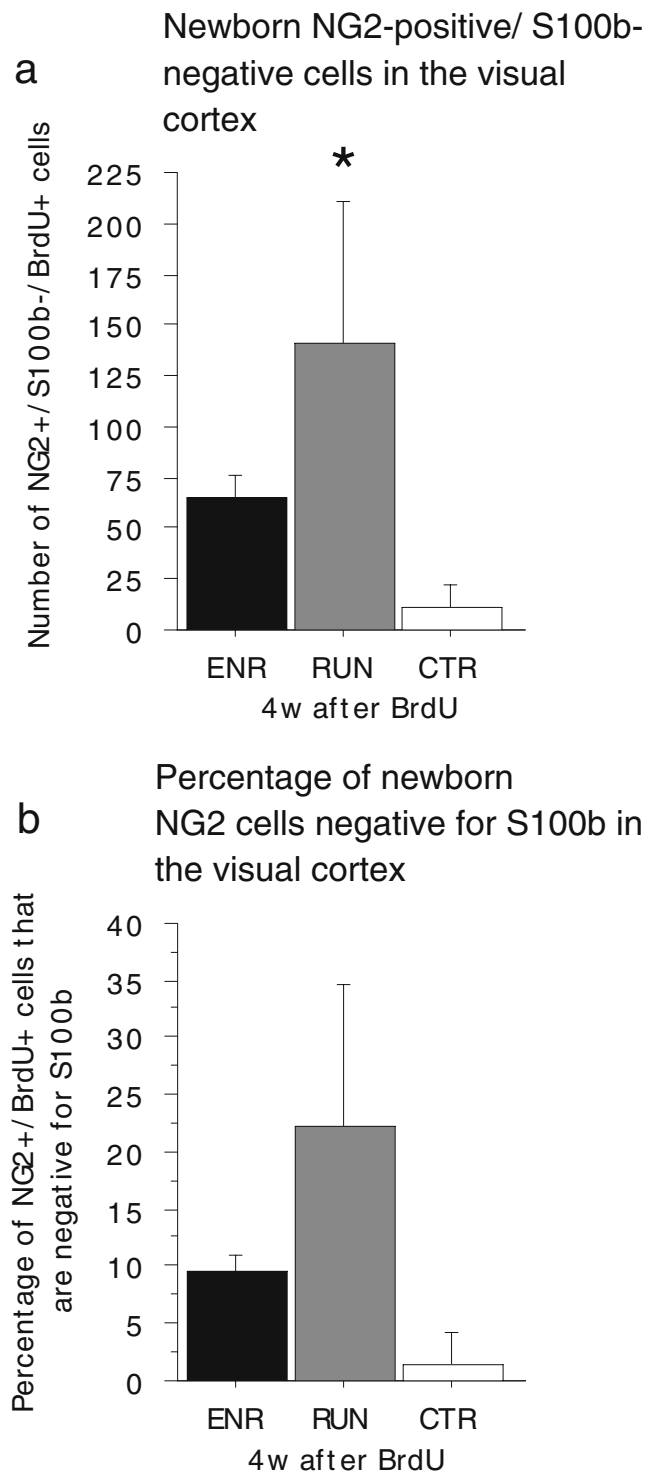
not performed because the third channel was needed for NeuN to help to identify layers II/III of the visual cortex). As the vast majority of BrdU/S100β cells also expresses NG2, we estimated the number of BrdU/NG2-positive S100β-negative cells by subtracting the number of BrdU/S100β-positive cells from the number of BrdU/NG2-positive cells. At 4 weeks after BrdU, a significant difference was observed between groups in the number of BrdU/NG2-positive S100β-negative cells (Fig. 7; one-way ANOVA: F(2,14)=4.330; P=0.0344; RUN vs. CTR: P=0.0107; ENR vs. CTR: P=0.0972; ENR: n=7 mice, RUN: n=4 mice; CTR: n=6 mice) and a trend toward a difference in the proportion of BrdU/NG2-positive S100β-negative cells in layer II/III of the visual cortex (Fig. 7; one-way ANOVA: F(2,14)=3.306; P=0.0667). Taken together, these data suggest that NG2 cells in the visual cortex and amygdala respond to ENR and/or RUN by down-regulating S100β expression.

Discussion

In the present study, we have found that NG2-positive cells in the amygdala show low levels of proliferation, limited change over time, and a striking antigen expression pattern that combines neuronal and glial immunocytochemical properties. A subset of these cells displays physiological properties ascribed to oligodendroglial precursors in other parts of the brain. Kainic acid application evokes a "complex" response in NG2 cells, suggesting their functional participation in activity-dependent processes. Voluntary wheel running and living with environmental enrichment lead to a loss of S100β expression in newborn NG2 cells, possibly indicating an induction of oligodendroglial differentiation in these cells. Additionally, physical activity and environmental enrichment reduce the numbers of newborn microglia in the adult amygdala.

A confusing selection of attributes has been ascribed to NG2-positive cells, possibly reflecting the existence of substantially heterogeneous subpopulations (Butt et al. 2002; Horner et al. 2000; Nishiyama 2007; Stallcup 2002). In most areas of the postnatal brain, including the amygdala, NG2 cells constitute the largest proliferative cell fraction (Dawson et al. 2003; Horner et al. 2000; Wennstrom et al. 2004). Often regarded as precursor cells committed to the oligodendroglial lineage, proliferating NG2-positive cells occur in the gray and white matter, consistent with an astrocytic and oligodendroglial differentiation potential (Zhu et al. 2008). In agreement with prior studies (Dawson et al. 2003), we here find that newborn NG2 cells largely persist in the NG2-positive state (at least over a period of 4 weeks after cell division).

Only a few BrdU-labeled cells express CNPase at 1 day and 4 weeks after BrdU, suggesting that the differentiation

Newborn NG2-positive/ S100b-negative cells in the visual cortex

a

Percentage of newborn NG2 cells negative for S100b in the visual cortex

b

Fig. 7 Environmental enrichment (*ENR*)/physical activity (*RUN*) regulate the number of BrdU/NG2-positive S100β-negative cells in layers II/III of the visual cortex (*CTR* control). **a** At 4 weeks after BrdU, a significant increase is found in the number of BrdU/NG2-positive S100β-negaitve cells in layers II/III of visual cortex of RUN and a trend toward an increase in ENR. **b** Proportion of BrdU/NG2-positive cells negative for S100β in visual cortex layers II/III at 4 weeks after BrdU (*error bars* SEM). *P<0.05

of newborn NG2 cells into mature oligodendrocytes occurs only on a minute scale. In a parallel study, we have followed the development of BrdU-positive cells in the amygdala over a much longer time period (up to 1 year). Although not enough material is available for an exhaustive quantification, we have noted that, by 6 months, about 50% (21 out of 40) of BrdU-positive cells in the amygdala are CNPase-positive (compared with 1.2% by 1 day and 6.3% by 4 weeks after BrdU). We cannot rule out that these changes are caused by the loss of BrdU incorporation by dilution below the threshold of detection (Hayes and Nowakowski 2002) in dividing (NG2-positive) cells and its persistence in non-dividing (CNPase-positive) cells. Alternatively, however, a subpopulation of NG2-positive cells might differentiate extremely slowly into myelinating oligodendrocytes.

NG2-positive cells share several characteristics with neuronal cells, such as synaptic input, calcium-dependent neurotransmitter release, and the expression of "neuronal" genes (Bergles et al. 2000; Ge et al. 2006; Matthias et al. 2003). Shared functional features should predict a shared pool of expressed genes specific to neurons and NG2-positive cells, but not other glia. Consistent with this notion, we have found "neuronal" antigens Doublecortin and NeuroD to be expressed in NG2-positive cells (but not postmitotic neuronal marker NeuN). PSA-NCAM is expressed in the adult amygdala (Nacher et al. 2002) and shows overlap with Doublecortin, but we have not found PSA-NCAM in BrdU-labeled cells. Doublecortin expression is considerably lower than in other Doublecortin-positive cell populations (such as cells in the dentate gyrus) and is confined to a cytoplasmic rim and proximal cell processes. As in one other report (Park et al. 2006), we have been unable to confirm reports on neurogenesis in the adult amygdala (Bernier et al. 2002; Fowler et al. 2002).

We have previously demonstrated the expression of an AMPA/kainate-type glutamate receptor in oligodendrocyte precursor cells identified by their characteristic morphology and their voltage-gated currents (Borges et al. 1994; Sontheimer et al. 1989). In the current study, we show that NG2 cells in the adult amygdala and oligodendrocyte precursors in the corpus callosum of the early postnatal brain have similar morphological and electrophysiological features to NG2 cells in the adult hippocampus (Bergles et al. 2000; Ge et al. 2006; Lin and Bergles 2004). To our knowledge, this is the first report that kainic acid evokes a complex response in NG2-positive cells. "Complex" responses are characterized by a rapid and long-lasting blockade of the resting K^+ conductance, a transient cationic current, and with a significant delay, a transient increase of an outwardly directed K^+ conductance. NG2 cells receive direct synaptic inputs from neurons (Bergles et al. 2000; Lin and Bergles 2004). Ge and colleagues (2006) have

reported that the synapses between neurons and NG2 cells are capable of undergoing activity-dependent modifications analogous to LTP at excitatory synapses. These modifications are mediated by Ca^{2+}-permeable AMPA receptors. Based on the findings in this study, we conclude that NG2-expressing cells in the amygdala express functional AMPA/kainate receptors.

We here report that life in an ENR and plenty of physical activity decrease the number of newborn microglia in the amygdala at 4 weeks after BrdU but do not significantly alter the number of newborn NG2–positive cells in the amygdala as compared with controls. A recent study by Okuda et al. (2009) has reported an increased density of BrdU-positive cells in the amygdala in a group of mice exposed to an ENR; in contrast to the present work (the first BrdU injection was given after 30 days in ENR), their study aimed at assessing the effect of an ENR on cells that were born prior to the exposure to ENR (dividing cells were labeled with BrdU before exposure to ENR). More importantly, however, as only cell densities were reported in this study, and as no cell counting according to stereological principles was performed, no assessment is possible with regard to the way that the actual numbers of newborn cells are changed by experimental intervention.

ENR and RUN increase the fraction of BrdU/NG2-positive cells that do not co-express S100β at 4 weeks after BrdU; this suggests a loss of S100β expression in newborn NG2 cells. S100β is a calcium-binding protein of the EF-hand family, participating in the regulation of a wide range of cellular processes with potential relevance for NG2 cell function (Donato et al. 2009). For instance, S100β expression in oligodendroglial precursors is correlated with their differentiation into myelinating oligodendrocytes, but mature oligodendrocytes no longer express S100β (Deloulme et al. 2004). Thus, the transient S100β expression in a subset of NG2-positive cells in our study might reflect cellular differentiation and maturation processes, such as differentiation to an oligodendroglial phenotype. Accordingly, the increase in the proportion of newborn NG2 cells lacking S100β at 4 weeks after BrdU might reflect an accelerated maturation of NG2-positive cells into myelinating oligodendrocytes under ENR and RUN conditions. In agreement with this interpretation, early reports indicated that ENR increases the density of oligodendrocytes in the posterior neocortex (Diamond et al. 1966; Szeligo and Leblond 1977). A modulation of oligodendrogenesis by ENR and RUN might be part of an adaptive process that includes neuronal changes and results in the refinement of existing neural circuitry. We may not have detected a parallel increase in the number of newborn mature oligodendrocytes (as determined by CNPas immunoreactivity), as the onset of CNPase expression might not take place within the 4 weeks after BrdU (also see above).

An important goal for future studies will be to determine whether ENR/RUN leads to an increase in CNPase-positive newborn cells in the amygdala/cortex at later time points after BrdU.

Our study has focused on the regulation of S100β in proliferating glial cells. In future studies, a systematic assessment of the effects of ENR and RUN on S100β abundance in various cell populations and extracellular compartments in the adult brain might be worthwhile. In addition to intracellular regulatory roles, S100β is secreted and exerts paracrine effects on other cell populations, including neurons (Donato et al. 2009). Knock-out of S100β in mice promotes LTP and leads to learning and memory enhancements relative to wild-type control animals (Nishiyama et al. 2002), suggesting that physiological levels of S100β constrain synaptic plasticity and memory formation. Accordingly, a possible broader down-regulation of S100β by ENR and RUN might contribute to the effects that these manipulations have on synaptic plasticity and memory (van Praag et al. 2000). Notably, however, the S100β knock-out effects on synaptic plasticity might largely be attributable to a reduction of extracellular S100β, as the perfusion of S100β mutant slices with recombinant S100β protein restores LTP enhancement (Nishiyama et al. 2002). Nevertheless, the down-regulation of S100β in NG2 cells by ENR/RUN might be related to or might parallel functional modifications that take place within NG2 cells, and that are unrelated to cell differentiation. Further studies should explore to what extent physiological properties of NG2 cells and the synaptic input onto these cells (Bergles et al. 2000; Ge et al. 2006; Lin and Bergles 2004) can be modified by ENR and/or RUN.

References

Arsenijevic Y, Villemure JG, Brunet JF, Bloch JJ, Deglon N, Kostic C, Zurn A, Aebischer P (2001) Isolation of multipotent neural precursors residing in the cortex of the adult human brain. Exp Neurol 170:48–62

Belachew S, Chittajallu R, Aguirre AA, Yuan X, Kirby M, Anderson S, Gallo V (2003) Postnatal NG2 proteoglycan-expressing progenitor cells are intrinsically multipotent and generate functional neurons. J Cell Biol 161:169–186

Bennett EL, Diamond MC, Krech D, Rosenzweig MR (1964) Chemical and anatomical plasticity brain. Science 146:610–619

Berger T, Schnitzer J, Kettenmann H (1991) Developmental changes in the membrane current pattern, K$^+$buffer capacity, and morphology of glial cells in the corpus callosum slice. J Neurosci 11:3008–3024

Bergles DE, Roberts JD, Somogyi P, Jahr CE (2000) Glutamatergic synapses on oligodendrocyte precursor cells in the hippocampus. Nature 405:187–191

Bernier PJ, Bedard A, Vinet J, Levesque M, Parent A (2002) Newly generated neurons in the amygdala and adjoining cortex of adult primates. Proc Natl Acad Sci USA 99:11464–11469

Blair HT, Schafe GE, Bauer EP, Rodrigues SM, LeDoux JE (2001) Synaptic plasticity in the lateral amygdala: a cellular hypothesis of fear conditioning. Learn Mem 8:229–242

Borges K, Ohlemeyer C, Trotter J, Kettenmann H (1994) AMPA/kainate receptor activation in murine oligodendrocyte precursor cells leads to activation of a cation conductance, calcium influx and blockade of delayed rectifying K$^+$channels. Neuroscience 63:135–149

Brown J, Cooper-Kuhn CM, Kempermann G, Praag H van, Winkler J, Gage FH, Kuhn HG (2003) Enriched environment and physical activity stimulate hippocampal but not olfactory bulb neurogenesis. Eur J Neurosci 17:2042–2046

Butt AM, Kiff J, Hubbard P, Berry M (2002) Synantocytes: new functions for novel NG2 expressing glia. J Neurocytol 31:551–565

Butt AM, Hamilton N, Hubbard P, Pugh M, Ibrahim M (2005) Synantocytes: the fifth element. J Anat 207:695–706

Dawson MR, Polito A, Levine JM, Reynolds R (2003) NG2-expressing glial progenitor cells: an abundant and widespread population of cycling cells in the adult rat CNS. Mol Cell Neurosci 24:476–488

Deloulme JC, Raponi E, Gentil BJ, Bertacchi N, Marks A, Labourdette G, Baudier J (2004) Nuclear expression of S100B in oligodendrocyte progenitor cells correlates with differentiation toward the oligodendroglial lineage and modulates oligodendrocytes maturation. Mol Cell Neurosci 27:453–465

Deng W, Aimone JB, Gage FH (2010) New neurons and new memories: how does adult hippocampal neurogenesis affect learning and memory? Nat Rev Neurosci 11:339–350

Di Bello IC, Dawson MR, Levine JM, Reynolds R (1999) Generation of oligodendroglial progenitors in acute inflammatory demyelinating lesions of the rat brain stem is associated with demyelination rather than inflammation. J Neurocytol 28:365–381

Diamond MC, Krech D, Rosenzweig MR (1964) The effects of an enriched environment on the histology of the rat cerebral cortex. J Comp Neurol 123:111–120

Diamond MC, Law F, Rhodes H, Lindner B, Rosenzweig MR, Krech D, Bennett EL (1966) Increases in cortical depth and glia numbers in rats subjected to enriched environment. J Comp Neurol 128:117–126

Donato R, Sorci G, Riuzzi F, Arcuri C, Bianchi R, Brozzi F, Tubaro C, Giambanco I (2009) S100B's double life: intracellular regulator and extracellular signal. Biochim Biophys Acta 1793:1008–1022

Ehninger D, Kempermann G (2003) Regional effects of wheel running and environmental enrichment on cell genesis and microglia proliferation in the adult murine neocortex. Cereb Cortex 13:845–851

Filippov V, Kronenberg G, Pivneva T, Reuter K, Steiner B, Wang LP, Yamaguchi M, Kettenmann H, Kempermann G (2003) Subpopulation of nestin-expressing progenitor cells in the adult murine hippocampus shows electrophysiological and morphological characteristics of astrocytes. Mol Cell Neurosci 23:373–382

Fowler CD, Liu Y, Ouimet C, Wang Z (2002) The effects of social environment on adult neurogenesis in the female prairie vole. J Neurobiol 51:115–128

Ge WP, Yang XJ, Zhang Z, Wang HK, Shen W, Deng QD, Duan S (2006) Long-term potentiation of neuron-glia synapses mediated by Ca^{2+}-permeable AMPA receptors. Science 312:1533–1537

Greenough WT, Volkmar FR (1973) Pattern of dendritic branching in occipital cortex of rats reared in complex environments. Exp Neurol 40:491–504

Hamill OP, Marty A, Neher E, Sakmann B, Sigworth FJ (1981) Improved patch-clamp techniques for high-resolution current recording from cells and cell-free membrane patches. Pflugers Arch 391:85–100

Hayes NL, Nowakowski RS (2002) Dynamics of cell proliferation in the adult dentate gyrus of two inbred strains of mice. Brain Res Dev Brain Res 134:77–85

Horner PJ, Power AE, Kempermann G, Kuhn HG, Palmer TD, Winkler J, Thal LJ, Gage FH (2000) Proliferation and differentiation of progenitor cells throughout the intact adult rat spinal cord. J Neurosci 20:2218–2228

Imayoshi I, Sakamoto M, Ohtsuka T, Takao K, Miyakawa T, Yamaguchi M, Mori K, Ikeda T, Itohara S, Kageyama R (2008) Roles of continuous neurogenesis in the structural and functional integrity of the adult forebrain. Nat Neurosci 11:1153–1161

Kempermann G, Kuhn HG, Gage FH (1997) More hippocampal neurons in adult mice living in an enriched environment. Nature 386:493–495

Kempermann G, Gast D, Kronenberg G, Yamaguchi M, Gage FH (2003) Early determination and long-term persistence of adult-generated new neurons in the hippocampus of mice. Development 130:391–399

Kronenberg G, Wang LP, Geraerts M, Babu H, Synowitz M, Vicens P, Lutsch G, Glass R, Yamaguchi M, Baekelandt V, Debyser Z, Kettenmann H, Kempermann G (2007) Local origin and activity-dependent generation of nestin-expressing protoplasmic astrocytes in CA1. Brain Struct Funct 212:19–35

Levine JM, Nishiyama A (1996) The NG2 chondroitin sulfate proteoglycan: a multifunctional proteoglycan associated with immature cells. Perspect Dev Neurobiol 3:245–259

Levison SW, Young GM, Goldman JE (1999) Cycling cells in the adult rat neocortex preferentially generate oligodendroglia. J Neurosci Res 57:435–446

Lin SC, Bergles DE (2004) Synaptic signaling between GABAergic interneurons and oligodendrocyte precursor cells in the hippocampus. Nat Neurosci 7:24–32

Maren S (2005) Building and burying fear memories in the brain. Neuroscientist 11:89–99

Maren S, Quirk GJ (2004) Neuronal signalling of fear memory. Nat Rev Neurosci 5:844–852

Matthias K, Kirchhoff F, Seifert G, Huttmann K, Matyash M, Kettenmann H, Steinhauser C (2003) Segregated expression of AMPA-type glutamate receptors and glutamate transporters defines distinct astrocyte populations in the mouse hippocampus. J Neurosci 23:1750–1758

Nacher J, Lanuza E, McEwen BS (2002) Distribution of PSA-NCAM expression in the amygdala of the adult rat. Neuroscience 113:479–484

Nishiyama A (2007) Polydendrocytes: NG2 cells with many roles in development and repair of the CNS. Neuroscientist 13:62–76

Nishiyama H, Knopfel T, Endo S, Itohara S (2002) Glial protein S100B modulates long-term neuronal synaptic plasticity. Proc Natl Acad Sci USA 99:4037–4042

Okuda H, Tatsumi K, Makinodan M, Yamauchi T, Kishimoto T, Wanaka A (2009) Environmental enrichment stimulates progenitor cell proliferation in the amygdala. J Neurosci Res 87:3546–3553

Palmer TD, Ray J, Gage FH (1995) FGF-2-responsive neuronal progenitors reside in proliferative and quiescent regions of the adult rodent brain. Mol Cell Neurosci 6:474–486

Park JH, Cho H, Kim H, Kim K (2006) Repeated brief epileptic seizures by pentylenetetrazole cause neurodegeneration and promote neurogenesis in discrete brain regions of freely moving adult rats. Neuroscience 140:673–684

Peters A (2004) A fourth type of neuroglial cell in the adult central nervous system. J Neurocytol 33:345–357

Praag H van, Kempermann G, Gage FH (1999) Running increases cell proliferation and neurogenesis in the adult mouse dentate gyrus. Nat Neurosci 2:266–270

Praag H van, Kempermann G, Gage FH (2000) Neural consequences of environmental enrichment. Nat Rev Neurosci 1:191–198

Raff MC, Miller RH, Noble M (1983) A glial progenitor cell that develops in vitro into an astrocyte or an oligodendrocyte depending on culture medium. Nature 303:390–396

Revest JM, Dupret D, Koehl M, Funk-Reiter C, Grosjean N, Piazza PV, Abrous DN (2009) Adult hippocampal neurogenesis is involved in anxiety-related behaviors. Mol Psychiatry 14:959–967

Reynolds R, Dawson M, Papadopoulos D, Polito A, Di Bello IC, Pham-Dinh D, Levine J (2002) The response of NG2-expressing oligodendrocyte progenitors to demyelination in MOG-EAE and MS. J Neurocytol 31:523–536

Rioult-Pedotti MS, Friedman D, Hess G, Donoghue JP (1998) Strengthening of horizontal cortical connections following skill learning. Nat Neurosci 1:230–234

Rosen GD, Williams AG, Capra JA, Connolly MT, Cruz B, Lu L, Airey DC, Kulkarni K, Williams RW (2000) The mouse brain library @ www.mbl.org. Int Mouse Genome Conference 14: 166 (www.mbl.org)

Sellers DL, Horner PJ (2005) Instructive niches: environmental instructions that confound NG2 proteoglycan expression and the fate-restriction of CNS progenitors. J Anat 207:727–734

Sirevaag AM, Greenough WT (1985) Differential rearing effects on rat visual cortex synapses. II. Synaptic morphometry. Brain Res 351:215–226

Sirevaag AM, Greenough WT (1991) Plasticity of GFAP-immunoreactive astrocyte size and number in visual cortex of rats reared in complex environments. Brain Res 540:273–278

Sontheimer H, Trotter J, Schachner M, Kettenmann H (1989) Channel expression correlates with differentiation stage during the development of oligodendrocytes from their precursor cells in culture. Neuron 2:1135–1145

Stallcup WB (2002) The NG2 proteoglycan: past insights and future prospects. J Neurocytol 31:423–435

Szeligo F, Leblond CP (1977) Response of the three main types of glial cells of cortex and corpus callosum in rats handled during suckling or exposed to enriched, control and impoverished environments following weaning. J Comp Neurol 172:247–263

Turner AM, Greenough WT (1985) Differential rearing effects on rat visual cortex synapses. I. Synaptic and neuronal density and synapses per neuron. Brain Res 329:195–203

Walsh RN (1981) Effects of environmental complexity and deprivation on brain anatomy and histology: a review. Int J Neurosci 12:33–51

Wennstrom M, Hellsten J, Tingstrom A (2004) Electroconvulsive seizures induce proliferation of NG2-expressing glial cells in adult rat amygdala. Biol Psychiatry 55:464–471

Wilson SS, Baetge EE, Stallcup WB (1981) Antisera specific for cell lines with mixed neuronal and glial properties. Dev Biol 83:146–153

Yamaguchi M, Saito H, Suzuki M, Mori K (2000) Visualization of neurogenesis in the central nervous system using Nestin promoter-GFP transgenic mice. NeuroReport 11:1991–1996

Zhu X, Bergles DE, Nishiyama A (2008) NG2 cells generate both oligodendrocytes and gray matter astrocytes. Development 135:145–157